

Liquid Crystal – Ferrofluid Dispersion

A dissertation submitted to The University of Manchester for the
degree of Master of Science by Research
in the Faculty of Science and Engineering

2018

Susumu Yoshida

School of Physics and Astronomy

List of Contents

Abstract	7
Declaration	8
Copyright Statement	9
1 Introduction	11
1-1 Liquid Crystals	17
1-2 Defects	24
1-3 Ferrofluid	29
2 Experimental Methods	31
2-1 Isotropic Liquid	31
2-2 Liquid Crystal.....	35
2-3 Magnets	37
2-4 Error	40
3 Isotropic Liquid Results and Discussion	42
3-1 Glycerine	44
3-2 Water	52
3-3 Silicone Oil.....	55
4 Liquid Crystal Results and Discussion	58
4-1 Size Dependency	58

4-2 Anisotropy.....	64
4-3 Different Strength of Magnetic Field.....	67
4-4 Gap Dependency.....	69
4-5 Temperature Dependency.....	71
5 Conclusion and Outlook	76
Acknowledgement.....	78
Reference.....	79

Word count: 10,499

Lists of Figures

Figure 1 Nematic multiple emulsion	12
Figure 2 A couple of ferrofluid droplets in LCs under a magnetic field	14
Figure 3 Molecular ordering in isotropic and anisotropic liquids.....	17
Figure 4 Molecular ordering in Nematics and Smectics	18
Figure 5 Angle between the molecules and the director	19
Figure 6 Two types of the boundary condition.....	22
Figure 7 Three types of the distortion	23
Figure 8 Director around the defect	25
Figure 9 Schlieren texture	26
Figure 10 Hedgehog and Saturn ring defects.....	28
Figure 11 Spike effect of ferrofluids.....	30
Figure 12 Magnetization curve of the ferrofluid	30
Figure 13 Sandwich cell preparation.....	33
Figure 14 Magnetic flux density of magnets.....	37
Figure 15 Photos of ferrofluid droplets in glycerine	44
Figure 16 Droplet motions in glycerine.....	45
Figure 17 Speed of the droplets in glycerine	46
Figure 18 Magnetic moments of ferrofluids	47

Figure 19 Droplet motions in water	52
Figure 20 Droplet motions in silicone oil	55
Figure 21 Photos of 5CB – ferrofluid dispersion	59
Figure 22 Droplet motions in 5CB	60
Figure 23 Photo of the droplet motions in 5CB	62
Figure 24 Anisotropy	64
Figure 25 Literature value of temperature dependence of the 5CB viscosity	66
Figure 26 Speed of the droplet in 5CB versus the strength of magnetic fields	67
Figure 27 Photos of temperature dependency of 5CB	72
Figure 28 Droplet motions at several temperatures	73
Figure 29 Experimental results of temperature dependency.....	74

List of Tables

Table 1 Strengths of magnetic fields of two types of Magnet.....	39
Table 2 Measurement error	41
Table 3 Speed and the thickness of boundary layer in glycerine	50
Table 4 Viscosity of glycerine	51
Table 5 Speed and the thickness of boundary layer in water.....	53
Table 6 Viscosity of water	54
Table 7 Speed and the thickness of boundary layer in silicone oil	56
Table 8 Viscosity of silicone oil.....	56
Table 9 Speed and the thickness of boundary layer in 5CB.....	61
Table 10 Viscosity of 5CB	61
Table 11 Anisotropy	65
Table 12 Magnetic field dependency	68
Table 13 Cell gap dependency	69
Table 14 Temperature dependency.....	74

Abstract

This research is aimed to determine the viscosity of liquid crystals by observing the motions of ferrofluid droplets in liquid crystal hosts under external magnetic fields. The ferrofluid droplets of size 20~30 μm were suspended in two plates covering the host liquid, and their motions under the magnetic field were observed with using a polarizing microscope. As the first step, three types of isotropic liquids, such as water, glycerin, and silicone oil, were employed as the host liquid. The speed of the moving droplet was much slower than the theoretical value calculated by the equilibrium between the magnetic force and the viscous force. This fact led us to one assumption, which the droplets involve the boundary layers under the magnetic field, and all results of isotropic liquids supported this fact. The main experiments of this research, using 4-cyano-4'-pentylbiphenyl (5CB), were conducted, and the result also supported the assumption above mentioned, which the new method to determine the 5CB viscosity was established. The experiments were conducted with several conditions, and unique anisotropic properties of 5CB were observed with this new method. This research showed that that the new method enables us to observe anisotropic properties with the quantitative aspects.

Declaration

I hereby declare that no portion of the work referred to in the thesis has been submitted in support of an application for another degree or qualification of this or any other university or other institute of learning.

Copyright Statement

- i. The author of this thesis owns certain copyright or related rights in it and s/he has given The University of Manchester certain rights to use such Copyright, including for administrative purposes.
- ii. Copies of this thesis, either in full or in extracts and whether in hard or electronic copy, may be made only in accordance with the Copyright, Designs and Patents Act 1988 and regulations issued under it or, where appropriate, in accordance with licensing agreements which the University has from time to time. This page must form part of any such copies made.
- iii. The ownership of certain Copyright, patents, designs, trademarks and other intellectual property and any reproductions of copyright works in the thesis, for example graphs and tables, which may be described in this thesis, may not be owned by the author and may be owned by third parties. Such Intellectual Property and Reproductions cannot and must not be made available for use without the prior written permission of the owner of the relevant Intellectual Property and/or Reproductions.
- iv. Further information on the conditions under which disclosure, publication and commercialisation of this thesis, the Copyright and any Intellectual Property and/or Reproductions described in it may take place is available in the University IP Policy in any relevant Thesis restriction declarations

deposited in the University Library, The University Library's and in The University's policy on Presentation of Theses.

1 Introduction

Liquid Crystals (LCs) are well known as intermediate states of matter between the liquid state and the solid state [1]. Since they were discovered in 1888 by Friedrich Reinitzer [2], who was an Austrian Botanical physiologist, they have been studied in academic and industrial fields. One of their most striking applications is liquid crystal displays, which can be seen widely in modern devices, such as television displays, smartphones, and watches [3]. LCs have a wide range of applications in a variety of fields, such as the lasing, the painting, and the fibres [4][5][6]. The reason why LCs have attracted a lot of interest and had such various applications is their unique properties caused by their anisotropy. Since they have some degrees of the molecular ordering orientationally or/and positionally, they show anisotropy features in their fluid-dynamic, elastic and electromagnetic properties [7]. Ferrofluids are colloidal liquids which consist of magnetic nanoparticles suspended in a liquid carrier. In comparison with Liquid Crystals, Ferrofluids has a shorter history. Steve Papell succeeded in forming ferrofluids for NASA in 1963 [8]. Regarding their applications, they are used as seals in hard disk drive, the active damper of suspension, and a thermal conductor in loudspeaker [9].

The aim of this research was to determine the viscous properties of liquid crystals by observing the motions of ferrofluids in liquid crystal hosts under magnetic fields applied. This study is based on a paper written in 1997 by Philippe Poulin which is entitled ' Novel Colloidal Interactions in Anisotropic Fluids '[10]. In this paper, Poulin succeeded in forming stable water droplets in the nematic liquid crystal 4-cyano-4'-pentylbiphenyl, which is usually called as 5CB. Moreover, he discovered that water droplets self-assembled to form linear chains and showed defects, as shown in Figure 1.

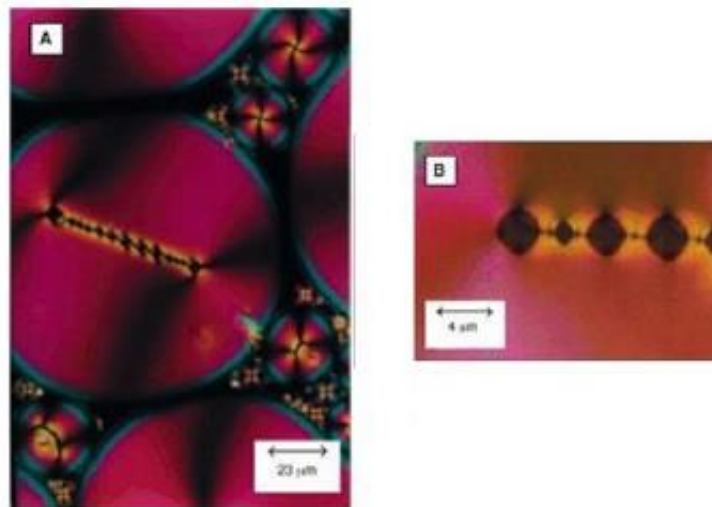


Figure 1: (A) Image of a nematic multiple emulsion taken under crossed polarizers. (B) A chain of water droplets under high magnification [10].

Figure 1-(A) shows that water droplets (1 to 5 μm in a diameter) were put in the larger nematic drops ($\sim 50 \mu\text{m}$ in a diameter) which were suspended in a continuous water host. We can see that the nematic parts are mainly coloured in red, while the isotropic parts including the small droplets and the host liquids appear black in this figure. He showed that the orientational elastic energy of 5CB based on the boundary condition in the director field at the nematic drop surface causes such colloidal interaction. This elastic energy has a long-range dipolar attraction and a short-range repulsion which cause the chain and the droplet spacing. Figure 1-(B) shows that the droplets were prevented from being close to each other[10].

Poulin reported that ferrofluids droplets were formed in a nematic liquid crystal in his paper, 'Direct Measurement of Colloidal Forces in an Anisotropic Solvent, which is published in collaboration with V. Caubuil and D.A. Weitz in 1997 [11]. Poulin showed that a pair of droplets linked together by topological defects appeared. When a magnetic field was applied to the system, large magnetic dipoles were induced within the droplets which forced the droplets apart from each other, as shown in Figure 2(a)-(c).

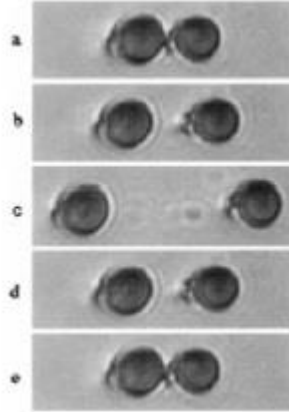


Figure 2: (a)-(b):Ferrofluid droplets being pushed apart by dipole-dipole repulsion by an external magnetic field. (c): External magnetic field removed. (d)-(e): Particles being pulled back together by elastic forces after the magnetic field was removed [11].

After the magnetic field was removed, an attractive force making the droplets closer to each other occurred between the droplets, which it was caused by the elastic properties of the liquid crystal(Figure 2 (d),(e)). Their system was viscously damped, and the attractive elastic force between droplets, F_a , could be determined by using the particles velocity and the effective viscosity of the liquid crystal, η_{eff} ;

$$m\ddot{r} = 2F_a(r) - 6\pi\eta_{eff}a\dot{r} , \quad (1)$$

where a is the droplet radius, m is their mass, \dot{r} is the velocity of the droplet [11].

In terms of the viscosity of liquid crystal, Miesowicz showed that the nematic liquid crystals have the anisotropy of the viscosity as well as the other properties in 1936 [12][13]. There are some papers which support this fact with the experimental result [14][15]. In particular, Chmielewski succeeded in measuring the viscosity of 5CB and observing its anisotropy and temperature dependency by using the slot viscometer [14].

Employing these previous studies, this research has been aimed to establish a new microscopic method to determine the viscosities of the liquid crystals. We have expected that the viscosities of the liquid crystals would be determined by observing the motion of the ferrofluid droplets under a magnetic field in the liquid crystal host and taking the balance between the magnetic force and the viscous force into consideration. The results of this research have been roughly categorized into two sections. The first one is to observe the motion of the ferrofluid droplets under a magnetic field within isotropic liquids. This part is aimed to establish the methods of preparing the droplets in the host liquid and determining the viscosities. The second part is to observe the motion in anisotropic liquids and determine the viscous properties of the liquid crystals.

In the following parts of this paper, some of the background theory behind ferrofluids and liquid crystals will be described. Then, this paper will explain the experimental techniques which are used for preparing samples and observing the motion of the droplets. The results and discussion will also be shown after that section.

1 -1 Liquid Crystals

The molecules in the crystal state are ordered orientationally and positionally whereas the molecules in the liquid state are not ordered and diffuse randomly. Liquid Crystals refer to an intermediate state of matter between the liquid state and the solid state because the molecules in liquid crystals show some degrees of orientational and/or positional orders while they diffuse like the molecules in the liquid state [6] (Figure 3).

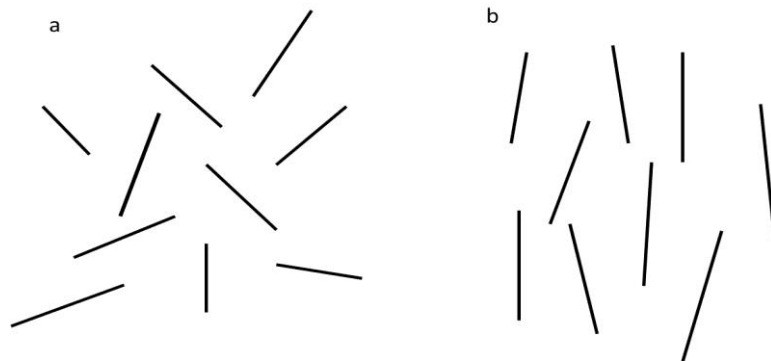


Figure 3: Schematics of the molecular ordering in isotropic liquid (a) and in a nematic liquid crystal (b)

Liquid crystals are categorized into two types; thermotropic liquid crystals and lyotropic liquid crystals. Thermotropic means that the transition of liquid crystal phases depends on the temperature and the phases exist within a certain temperature range. On the other hand, lyotropic liquid crystals are often formed by dissolving amphiphilic molecules in a suitable solvent. The liquid crystal phase exists in a certain range of concentration. We will focus on thermotropic liquid crystals because only thermotropic liquid crystals are employed in this research.

There are numerous phases in thermotropic liquid crystals, such as nematic, smectic A, smectic C, etc. Figure 4 shows a schematic of the molecular ordering in main phases of thermotropic liquid crystals.

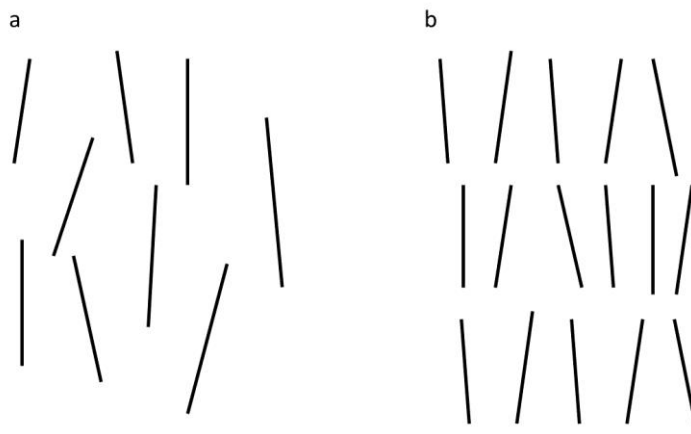


Figure 4: A schematic of the molecular ordering in (a) Nematics, (b) Smectic

In the nematic phase, the molecules have the only orientational order and no positional order, which the name is based on the Greek word [6]. The smectic phases, on the other hand, have one orientational order and the positional order due to the arrangement of molecules in layers. They usually appear at the lower temperature than the nematic phase. In this research, the only 5CB, which is a nematic liquid crystal, was used. The orientational order of a nematic liquid crystal can be defined by the order parameter, P ;

$$P_2 = \frac{1}{2} \langle 3\cos^2\theta_i - 1 \rangle \quad (2)$$

Where i is the number of molecules and θ_i is the angle between the long axis of molecules in a nematic liquid crystal and the preferred direction [16]. Figure 5 shows this angle.

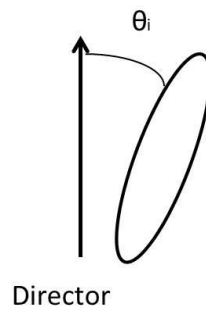


Figure 5: Diagram of θ_i .

The preferred direction of the molecules is written as the director, \hat{n} [17]. The value of an order parameter of the nematic liquid crystal is in a range from 0.3 to 0.8 [6]. The molecules in a nematic liquid crystal have the only orientational order and can freely flow as long as they maintain the director. When the system is heated, the molecules will lose their orientational order, and the fluid will be isotropic.

When the polarized light comes into the nematic liquid crystal, it is well known that birefringence occurs. Because of their anisotropy, liquid crystals have different refractive indexes for different directions of the polarized light. The polarized light can be split into two components. The first one is the ordinary component, which the plane of polarization is perpendicular to the direction of propagation, and the second one is the extraordinary component, which the plane is parallel to the direction of propagation [17]. In anisotropic materials, the speed of propagation is determined by the orientation of the plane of polarization in terms of the optic axis of the material. Two refractive indexes exist corresponding to the ordinary and extraordinary components, n_o is the index of the ordinary component while n_e is the index of the extraordinary component. The level of birefringence is given by,

$$\Delta n = n_e - n_o. \quad (3)$$

The value of Δn of a typical nematic liquid crystal is around 0.2 [6][18].

The boundary conditions of the nematic liquid crystal should be noted. In this research, the liquid crystal was placed between two glass surfaces. In this case, the preferred alignment of the molecules occurs. There are two basic forms of alignment for liquid crystalline compounds, homeotropic and homogeneous (planar). Homeotropic alignment is that the molecules in the nematic liquid crystal are oriented perpendicular to the surface. Thus, when the sample is observed by a polarizing microscope, polarized light is not affected by material and light could not be seen by an observer through the analyser. This alignment is obtained by coating a surface with a surfactant molecule. In planar alignment, the molecules in the nematic liquid crystal are oriented parallel to the surface. The planar alignment is obtained by coating a surface with a thin film and unidirectionally rubbing it to create grooves on the surface [19]. Figure 6 shows these alignments.

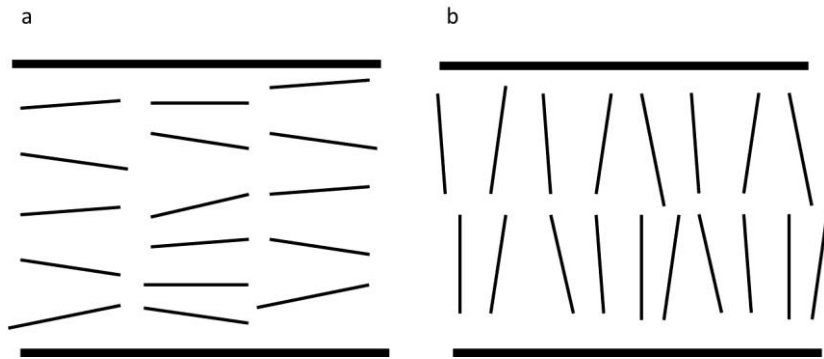


Figure 6: Models of two types of the alignments, planar (a), homeotropic (b).

Through the liquid crystalline material is confined under boundary conditions and the molecules are arranged in a particular order, the liquid crystals response to these forces as a distortion of the director. In particular, in nematic phases, three types of the distortion are common; splay, twist and bend. Figure 7 shows the models of these types of the distortion.

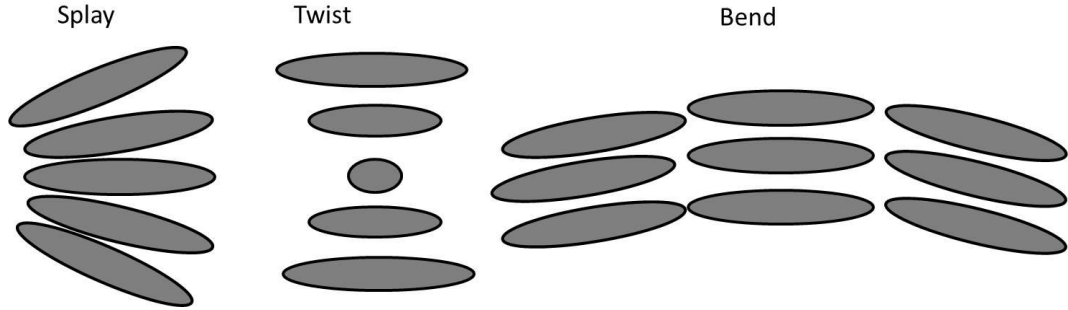


Figure 7: Illustrations of three types of the distortion.

Relating to the distortion, we should consider the free energy of varying spatial distortion of the director \hat{n} . The energy is determined by the Frank free energy, which describes the increase in the free energy density of a liquid crystal caused by distortions from its uniformly aligned configuration [20];

$$F = \frac{1}{2}K_1(\hat{n}(\nabla\hat{n}))^2 + \frac{1}{2}K_2(\hat{n}(\nabla \times \hat{n}))^2 + \frac{1}{2}K_3(\hat{n} \times (\nabla \times \hat{n}))^2 \quad (4)$$

where K_1, K_2, K_3 represent the splay, twist and bend coefficients respectively.

While the elastic modules of solids are written by the relationship between the distortion and stress, the elastic modules of nematic liquid crystals are described with the frank free energy coefficients, K_1, K_2, K_3 , corresponding to the type of the distortion.

1-2 Defects

In the liquid crystal, defects arise from foreign inclusions or by themselves, which break the symmetry structure of the surrounding director fields. Topological defects are caused by the phase transition and produce the break of the symmetry structure [21]. Since the thermotropic liquid crystals are regularly made by cooling or heating the material, defects often occur in the liquid crystal phases. These topological defects are often used to identify liquid crystal phases because such defects cause unique texture corresponding to the orientation of the molecules. The defects are regions where the director cannot be uniquely defined. Figure 8 shows some examples for the orientation of the director around a defect. The defects in liquid crystals have an effect on not only the local area nearby the defects but also the behaviour of a sample as a whole [22].

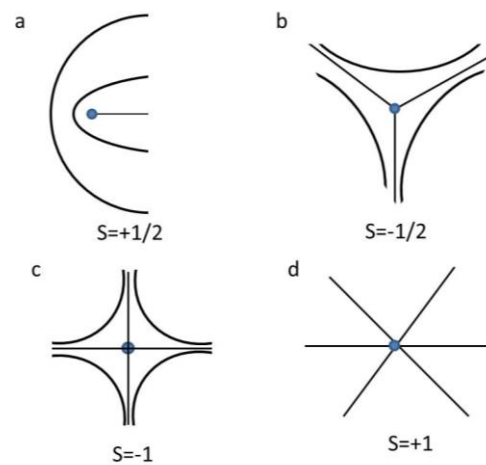


Figure 8: Diagrams of the orientations of the directors around the defect corresponding to each value of S .

Disclinations, which are line defects in the liquid crystals, are determined by their strength and charge. S represents the index for the strength and charge of defects. We can obtain the strength of the defect by determining to form a closed loop around the defect [23], which the value of S is determined by the number of times the director rotates through 2π . For example, if $S=\pm 1/2$, then the director rotates by π for one full loop around the disclination. If $S=\pm 1$, then the director rotates by 2π . We can also obtain the charge of defect, which shows that disclinations are able to cancel each other out or not, by seeing the sign of S . If S is positive, then the director rotates counter-clockwise in traversing a counter-clockwise path around disclination. If S is negative, the director rotates clockwise in traversing a counter-clockwise path around disclination.

Regarding the nematic liquid crystals, when cooling down from the isotropic liquid, the defects appear in the nematic liquid crystals. In addition, they exhibit the unique texture, which is that disclinations connected by black brushes, if the sample is thick enough and observed between crossed polarisers. This pattern is known as the Schlieren texture [6] and is shown in Figure 9. The Schlieren brushes appear black because of optical extinction caused by the crossed polarisers. To cause the optical extinction, the molecules have to be aligned in the direction of the either of the two crossed polarisers.

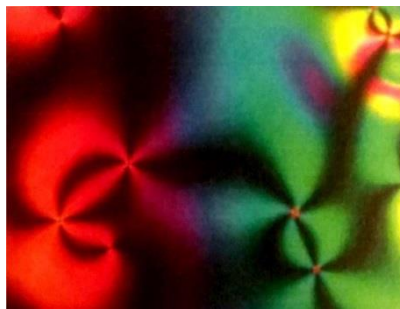


Figure 9: Image of Schlieren texture of 5CB [24].

As mentioned above, the strength S of a defect is given by determining a closed loop which forms around the defect. On the other hand, the strength S of a defect is determined by measuring the dark brushes seen in Figure 9. If there are four brushes connected with a defect, the defect has the strength $S=1$, and if

there are two brushes connected with a defect, the defect has the strength $S=1/2$. As the respect to the charge of S , if the brushes rotate in the same direction as the direction in which the crossed polarisers are rotated, the defect is positive. If the brushes rotate in the opposite direction, it means the defect is negative. Moreover, Defects of opposite charge and equal strength will attract each other and eventually annihilate, and it causes the same unique texture since the formation of defects will be changed by such interactions.

The defects are also created by putting the isotropic liquid droplets or the dispersion of colloids in the liquid crystal host. These methods have attracted interest since they show interesting properties, especially their unique textures when we observe them by a polarising microscope. In the previous studies, there are some representative examples of such textures; a point-like defect called Hedgehog [25], Saturn ring that surrounds a droplet as the name suggests [26], as shown in Figure 10.

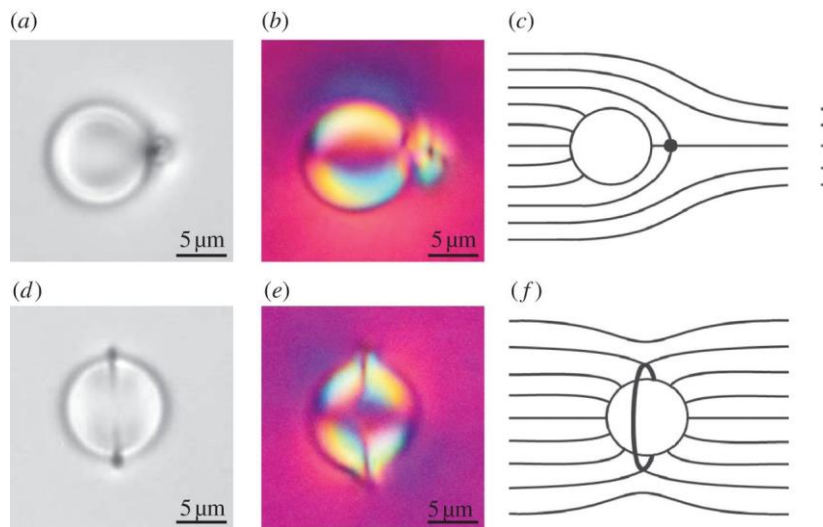


Figure 10: Pictures and Illustrations of Hedgehog defect and Saturn ring defect. A silica microsphere was treated so as to align the LC molecules perpendicular to its surface. Pictures of (a) and (d) were taken without polarizers while (b) and (e) were taken with crossed polarizers. (c) and (f) are schematics of the director configuration. (a-c) show the hedgehog defect, a black point shown in (a). (d-f) show the Saturn ring defect, a ring around the sphere shown in (d) and (e) [27].

1-3 Ferrofluid

Ferrofluids are liquid to be magnetized under magnetic fields, which consist of nano-sized magnetic particles held in a stable colloidal suspension in a liquid carrier, often water or oil [29]. Ferrofluids are composed of nanoscale particles, which its diameter usually ranges between 6 and 20um, and magnetite, hematite or iron are often used to form ferrofluids[9]. They are polymer coated or charged in order to prevent coagulation [9]. The composition of a typical ferrofluid is approximately 5vol% of particles, 10vol% of surfactant and 85vol% of the carrier. Ferrofluids are well known for their unique pattern formation under the magnetic field, one of them is called Spike Effect, shown in Figure 11. While they can be influenced by magnetic fields, they are not ferromagnetic in the strict sense, which means they show a magnetization only when magnetic fields are applied to them. Since they have the high magnetic susceptibility, they can be easily manipulated and controlled by magnetic fields. When the magnetic field is applied to ferrofluids, the magnetic force, F_k , is given by Kelvin's Law[30],

$$F_k = \mu_0 \int \vec{M} \nabla \vec{H} dV \quad (5)$$

Where μ_0 is the magnetic permeability of a vacuum, \vec{M} is the internal magnetization of the ferrofluids, and $\nabla\vec{H}$ is the magnetic fields gradient across the ferrofluids. Figure 12 shows the typical magnetization curve for the ferrofluid as a function of H.



Figure 11: A picture of spike effects of ferrofluid [31].

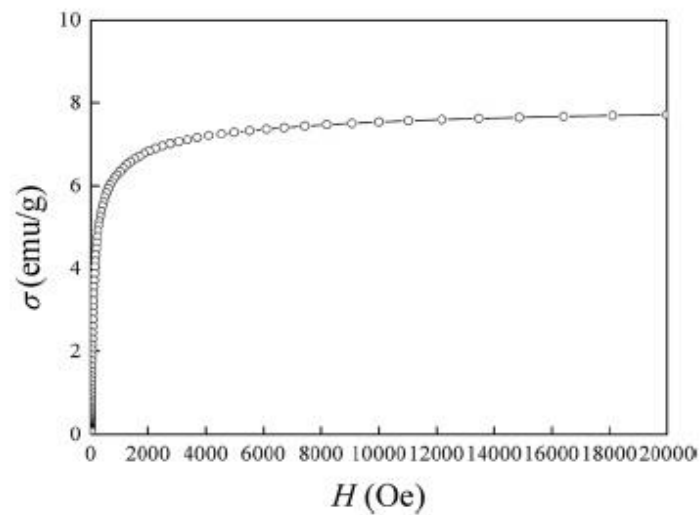


Figure 12: Magnetization curve of the ferrofluid (EMG807, Ferrotech, USA, at 300 K) [32].

2 Experimental Methods

2-1 Isotropic Liquid

These experiments, which employed the isotropic liquids and ferrofluids, were aimed to establish the methods of preparing the dispersion of the liquids and ferrofluids in which the droplets of ferrofluids were expected to be formed and the methods of determining the viscosities of liquids by observing the motions of the droplets under magnetic fields. The isotropic liquids employed in this research are water, glycerin, and silicone oil. Water is one of the simplest liquids and expected to be suitable for the first step to establish the methods of preparing the droplets in the liquid. Glycerin was employed in this experiment because it has been expected that the droplets of ferrofluids could be formed easily. The reason why silicone oil was employed is that silicone oil has a similar value of viscosity with 5CB, and is not water-soluble which is same as 5CB.

For these experiments, the two types of ferrofluids were used corresponding to solubility in water of each isotropic liquid. For water and glycerine, which are water-soluble liquid, the oil-based ferrofluid (EFH1, Ferrotech, USA) was used. The water-based ferrofluid (WHKS1S12, Liquid Research Ltd, UK) was used for

silicone oil. These isotropic liquids were used to form mixtures with each type of ferrofluids. Through several times of preparing samples, it was discovered that 0.1 vol% of ferrofluids is appropriate to form the droplets in host liquids. In terms of the methods of preparing mixtures, the mixtures were formed by putting ferrofluids in host liquids to make the concentration 0.1 vol% with the micropipettes, and then, the ultrasonic was applied to the mixture for 2 or 3 min by the sonicator(S0375 SONOMATIC, JENCONS, UK) in order to prepare the dispersion. The frequency of the ultrasonic was 40-50 Hz.

The cells containing the mixtures were created by the following steps. First, the glass was cut into small plates measuring 2.5x1.8 cm. Then, In order to clean the plates, the plates were placed in containers with distilled water and given ultrasonic by the sonicator for 15 min. The sonicator uses ultrasonic to displace contaminating particles from the surface. This step was repeated with the same plates in acetone and isopropyl alcohol. The next step was to create the sandwich cell. Two pieces of the spacer, which were cut into the appropriate size measuring 0.3x2.0 cm and its thickness was 100 μm , were sealed on the surface of one plate with UV glue as shown in Figure 13 (a). The UV glue used in this process is Norland Optical Adhesive 68 (NOA68, Norland Product Inc, USA). After the plate was exposed to ultraviolet light for 10 min in order to fix the spacer by

UV glue, the mixture was placed in the space between two pieces of the spacer by a pipette (Figure 13 (b)), which the amount of the mixture was around 80ml. Next, the other glass plate was placed on the plate on which the spacer and mixture were placed as shown in Figure 13 (c). The final step of cell preparation was that the cell was exposed to ultraviolet light for 10 min again after UV glue was used to coat the two other sides in order to seal the two plates together and the four sides around the mixture.

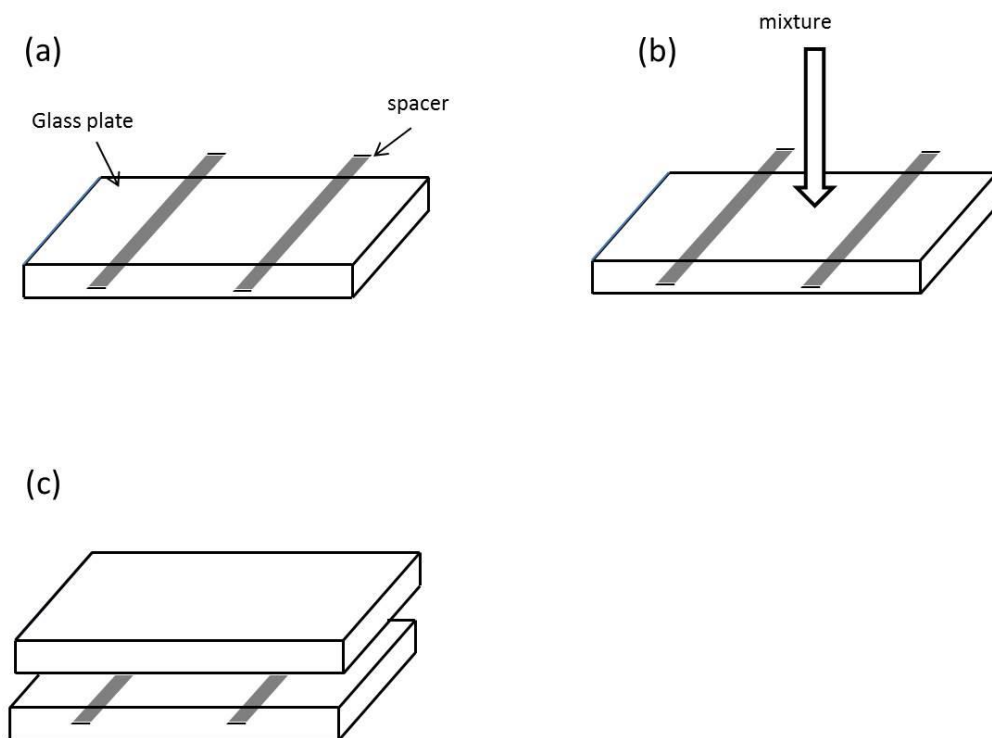
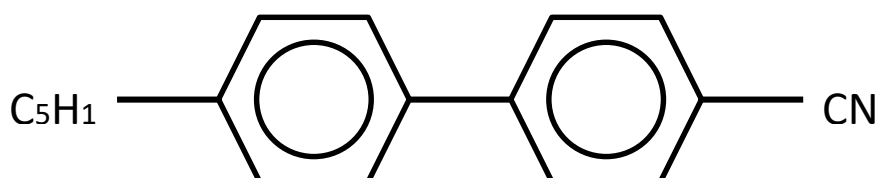


Figure 13: Diagram of sandwich cell preparation.

The experiment was conducted with following steps. The cells were placed on the microscope and applied with external the magnetic field by a permanent cylinder magnet, which the detail of magnets employed in this experiment will be shown in the following section. The two microscopes were used in this experiment; Nikon Optiphot Pol was used for water and glycerine, and Leica DMLP was for silicone oil. It was necessary to change the microscopes from Nikon one to Leica one because the Nikon one was in trouble. It was observed that the droplets in host liquids were moved by the magnetic field and the movie of such behaviour was taken with an imaging system (uEye CP) at a pixel resolution of 2048 x 1088 at a time resolution 0.1s. Snapshots were taken from the movie by intervals of a second. The data of the motion of the droplets was obtained by analyzing the position for each snapshot with using Image J (image processing software developed at the National Institutes of Health)[33][34]. All experiments in this section were conducted at room temperature, 25 °C.

2-2 Liquid Crystal

The liquid crystal employed in this research was 4-cyano-4'-pentylbiphenyl, which commonly is called as 5CB. 5CB is a standard liquid crystal material consisting of a single component and shows the nematic phase at room-temperature [6]:



The phase transition temperatures are given by Cryst 22 N 34 Iso [14]. The water-based ferrofluid was used in this experiment (WHKS1S12, Liquid Research Ltd, UK). The concentration of the mixture of 5CB and water-based ferrofluid was 0.1 vol% of the ferrofluid which is same as the concentration of the isotropic one. The dispersion of 5CB and the ferrofluid was formed by applying the ultrasonic (40-50 Hz) to the mixture with a sonicator for 3 min.

The method of cell preparation for 5CB – ferrofluid dispersion was same as the isotropic one without the step of the glass coating. The plates divided from the glass were spin-coated with polyvinyl alcohol. The plates were heated to 100 °C

for 15 min, and then spin-coated with PVA. After spin-coating, the plates were heated again to 100 °C for 15min. The plates were rubbed unidirectionally with a velvet cloth. These steps were conducted for aligning molecules in 5CB when 5CB is placed between two glass plates. The sandwich cells for 5CB were created with such spin-coated glass by the same methods as the isotropic one.

The cells were placed between crossed polarizers in a microscope (Leica DMLP) and external magnetic fields were applied to the cells. The experiments were conducted with several conditions, such as different sizes of droplets, directions of a magnetic field, strengths of magnetic fields, cell gaps, and temperature. The data was collected with same methods as the isotropic one.

2-3 Magnets

As the preparation for the above experiments, the magnetic fields caused by magnets used in the experiments were measured with a gauss meter (GM08, HIRST Magnetic Instruments Ltd) with an accuracy of $\pm 0.1\%$. Figure 14 shows the magnetic flux density of the magnets versus distance from the magnets. In the experiments, the two types of the magnet were used and were named magnet A and magnet B individually.

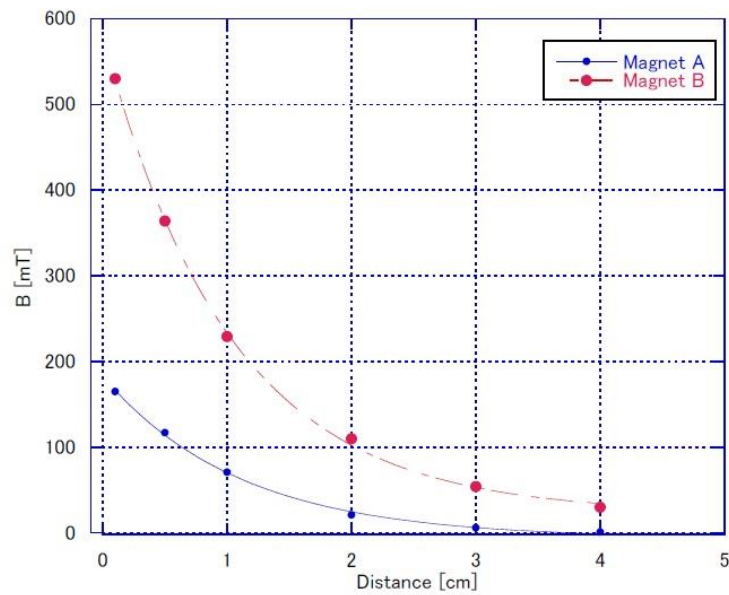


Figure 14: A graph of magnetic flux density B of two magnets as a function of distance from the magnets.

In this graph, the fitting curves were determined by using graph software (KaleidaGraph, HULINKS Inc., Japan), and the function of the fitting curves is given by,

$$B = a \cdot \exp(-b \cdot x) + c \quad (6)$$

Where a, b, and c are coefficients, and x is the distance from the magnet. In the experiments, five different values of distances from the magnets to the cell were used: 3.0, 2.5, 2.0, 1.5, 1.0 cm. The values of ∇B were determined by calculating the gradients of the equation (6) with the data, shown in Table 1. In the following sections, these values will be used for analysis.

Table 1: The values of the strength of magnetic fields for each value of distance.

	Magnet A $0.199 \cdot \exp(-96.6 \cdot x) - 0.0111$	Magnet B $0.557 \cdot \exp(-97.3 \cdot x) - 0.0000100$
[cm]	∇B [T/m]	∇B [T/m]
1	7.30	20.5
1.5	4.53	12.6
2	2.81	7.74
2.5	1.74	4.46
3	1.08	2.92

2-4 Error

Since the experiments were analysed by ImageJ, there are some possibilities that errors occurred in the step of measuring the values of diameter and position of the droplets in host liquids. The errors on such values, σ_x , were judged to be ± 5 pixels. In terms of the experiments with the Nikon microscope, which mean the experiments of glycerine and water, the width of the image in pixels was 2048 pixels and the width in μm was 572 μm . Thus, the error was determined to be $\pm 1.4 \mu\text{m}$. On the other hand, in the experiments with the Leica microscope, which means the experiments of silicone oil and 5CB, the width of the image in pixels was 2048 pixels, and the width in μm was 1575 μm . The error was determined to be $\pm 3.8 \mu\text{m}$. The movie of the droplet motions was taken for 8 seconds for the all experiments and there was no error on the value of time. To be simple, the errors on speed, σ_v , can be determined by $\sigma_v = \sigma_x/8$. The values are shown in Table 2.

Table 2: The values of σ_x , σ_v for each experiment.

	Glycerine, Water	Silicone oil, 5CB
σ_x [μm]	± 1.4	± 3.8
σ_v [$\mu\text{m}/\text{s}$]	± 0.18	± 0.48

3 Isotropic Liquid Results and Discussion

Before the results are shown, it should be noted how the viscosity of a liquid is determined by observing the motion of ferrofluid droplets. Under application of a magnetic field, a droplet in a host liquid reaches an equilibrium speed, v_{eq} . In such case, the magnetic force F_m should be equal to the viscous force F_s . The equation is given by:

$$V\mu_0 M_m \nabla H = 6\pi\gamma r v_{eq} \quad (7)$$

where V is the volume of the droplet, μ_0 is the magnetic vacuum susceptibility and equal to $4\pi \times 10^{-7} \text{ N/A}^2$, M_m is the mass magnetization, γ is the viscosity, and r is the droplet radius. ∇B can be approximated as $\nabla\mu_0 H$ for the non-ferromagnetic environment[30][35]. The viscosity can be obtained with the equation, $\rho M_m = M_{vol}$, where ρ is the density and M_{vol} is the volume magnetization:

$$\gamma = \frac{2r^2 M_{vol} \nabla B}{9v_{eq}} \quad (8)$$

This is the simplest way to determine the viscosity by the motion of a droplet, and it had been expected that the droplets would show behaviour following the equation (8) before the experiments were conducted.

In the following sections, the results of glycerin–ferrofluid dispersion will be described first. After that, the results of water and silicone oil will be shown.

3-1 Glycerine

Figure 15 shows the droplets formed in glycerine and their motions under magnetic fields. Magnet B was used in this experiment and the distance between Magnet B and the centre of the cell was 1.0 cm. From Figure 15, it can be seen that ferrofluid droplets in glycerine were moving under magnetic fields. Figure 16 shows the motions of 3 sizes droplets under magnetic fields as a function of time.

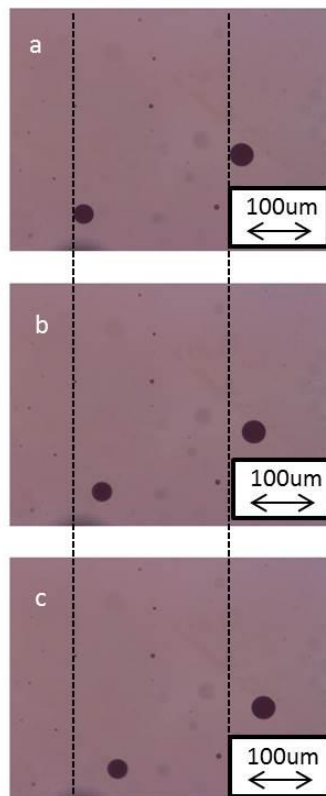


Figure 15: Photos of ferrofluid droplets in glycerine host: (b) 5 seconds after the moment of (a), (c) 10 seconds after.

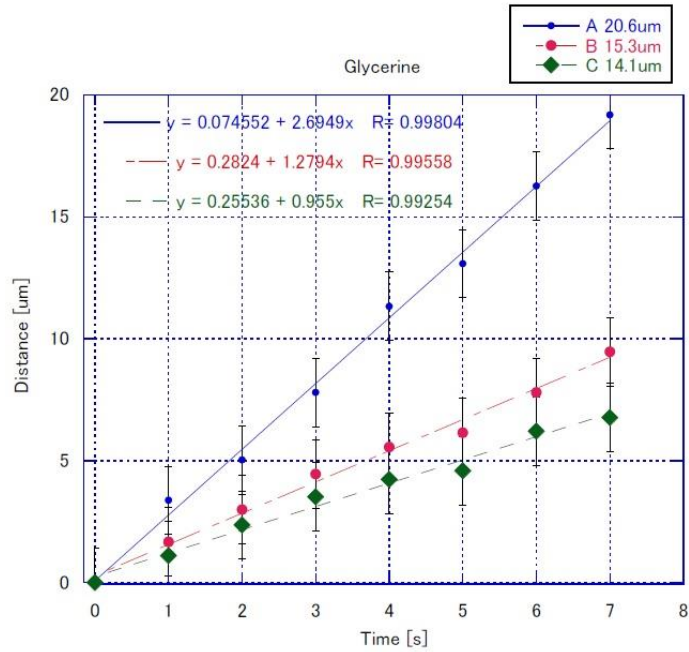


Figure 16: A graph of droplet motions in glycerine as a function of time, $\nabla B = 20.5 [T/m]$.

The diameter of the largest droplet was $20.6 \sigma_x \mu\text{m}$, while the second one is $15.3 \mu\text{m}$ and the smallest one is $14.1 \mu\text{m}$. In Figure 16, the larger droplets showed the faster speed. According to the theory mentioned above, the relationship between diameter and speed can be obtained by changing the formation of the equation (8):

$$v_{eq} = \frac{2r^2 M_{vol} \nabla B}{9\gamma} \quad (9)$$

In order to compare the results with the theory, the values of speed for each diameter were calculated by using the literature values, such as $\gamma = 0.90 \text{ Pa}\cdot\text{s}$ [36], $M_m = 7.0 \text{ T/kg}$ [32], $\rho = 1350 \text{ kg/L}$ which is based on the product data. In terms of M_m, ρ , these values will be employed in all the following parts. Figure 17 shows the differences of speed between the experimental results and the theory.

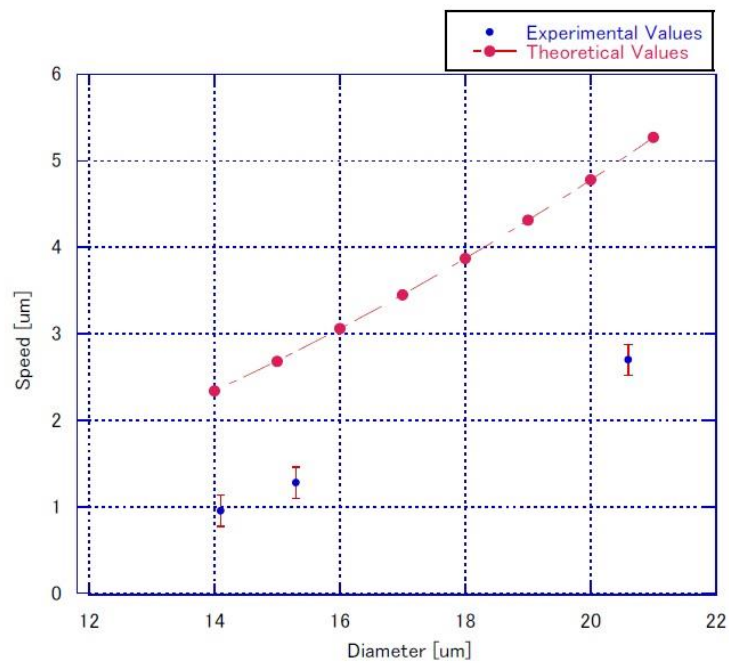


Figure 17: A graph of the speed of the droplets in glycerine as a function of diameter, $\nabla B=20.5 \text{ [T/m]}$.

It can be seen from this graph that the experimental values is quite small in comparison with the theoretical values, which are less than half of the theoretical values. This result was not satisfied with the theory absolutely. This fact means that the equation (8) was not suitable for this system and there is a necessity to establish the new method. Then, one assumption was considered, which there would be boundary layer in droplets and it influenced in the motion of droplets. To go into the detail, Figure 18 shows the schematic of the magnetic moments of molecules in a ferrofluid droplet.

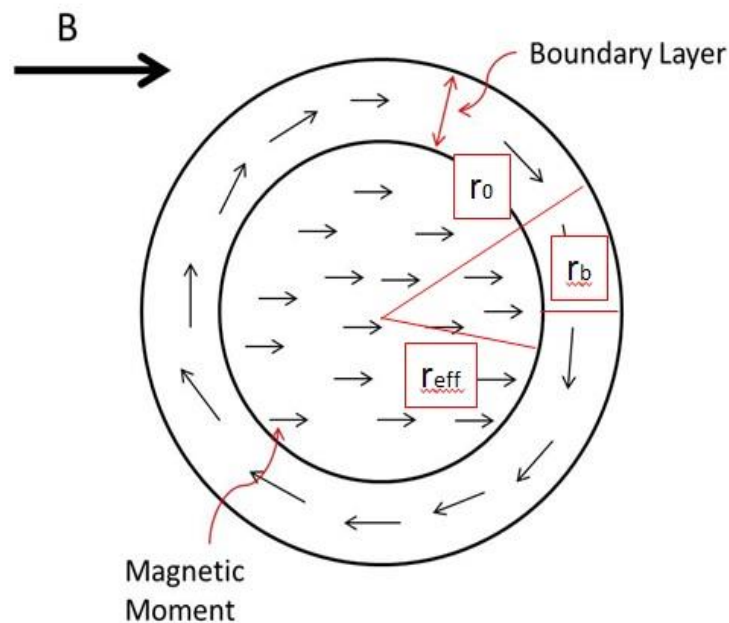


Figure 18: Schematic of the magnetic moments of molecules in a ferrofluid droplet.

In the core part of the droplets, the directions of the molecular magnetic moments are aligned to be parallel to the direction of the external magnetic fields. In the boundary layer, the directions of the molecular magnetic moments are not aligned and form the shape to negate the magnetic moments mutually. In this figure, the circle shape was employed for convenience sake. However, it should be noted that there are other possibilities. Since such a formation, the molecules in the boundary layer are not contributed to the magnetic force, F_m . To take this assumption into consideration, the magnetic force, F_m , is rewritten as the following:

$$F_{m1} = V_{eff} \mu_0 M_m \nabla H \quad (10)$$

where V_{eff} is the volume of a droplet excluding the boundary layer. F_{m1} should be equal to F_s :

$$V_{eff} \mu_0 M_m \nabla H = 6\pi\gamma r_0 v_{eq} \quad (11)$$

$$\gamma = \frac{2r_{eff}^3 M_{vol} \nabla B}{9r_0 v_{eq}} \quad (12)$$

where r_{eff} is the radius of a droplet excluding the thickness of the boundary layer, r_0 is the radius of a whole droplet. The value of r_b is expected to be constant for any size of droplets because of the size dependency of the speed shown in Figure 17.

By analyzing the data of glycerin, it can be confirmed whether this assumption is reasonable or not. As the steps to confirm the above assumption, the value of r_{eff} should be determined by the calculation of the equation (12) with the literature value of the viscosity. The literature values for the involved quantities are as follows: $\gamma = 0.90 \text{ Pa}\cdot\text{s}$ (25°C) [36], $M_m = 7.0 \text{ T/kg}$ [32], $\rho = 1350 \text{ kg/L}$ which is based on the product data. In terms of M_m, ρ , these values will be employed in all the following parts.

Table 3 shows the values of the speed for each size droplet, the values of r_{eff} , and the values of r_b which mean the thickness of the boundary layer.

Table 3: The values of Speed, r_{eff} , r_b for each size of the droplets in glycerine.

	A	B	C
Diameter [μm]	20.6	15.3	14.1
Speed [$\mu\text{m} / \text{s}$]	2.69	1.27	0.95
r_{eff} [μm]	8.34	5.89	5.20
r_b [μm]	1.97	1.74	1.84

According to Table 3, the three values of the thickness of the boundary layer for three sizes are similar to each other, and it is reasonable that the thickness of the boundary layer is $1.8 \mu\text{m}$, which the values are included approximately in the range of $\pm 10\%$ from $1.8 \mu\text{m}$.

On the other hand, the viscosity also can be determined by using that value, $r_b = 1.8 \mu\text{m}$. Table 4 shows the values of the viscosity for each sizes droplets calculated with the equation(12).

Table 4: The values of viscosity for each size of the droplets in glycerine, $r_b = 1.8\mu\text{m}$.

	A	B	C	Literature Value
Diameter [μm]	20.6	15.3	14.1	
Speed [$\mu\text{m} / \text{s}$]	2.69	1.27	0.95	
Viscosity [$\text{Pa}\cdot\text{s}$]	0.957	0.876	0.923	0.90

In comparison with the literature value, All droplets show quite similar values whose errors are approximately 5 %. From these results, the assumption above mentioned could be reasonable, and this method to determine the viscosity by observing the motion of the droplets is appropriate.

3-2 Water

In this experiment, Magnet A was used in this experiment and the distance between Magnet A and the centre of the cell was 2.5 cm. It is same as the experiment of glycerine that Oil-based ferrofluid was employed. Figure 19 shows the motions of the droplets under external magnetic field.

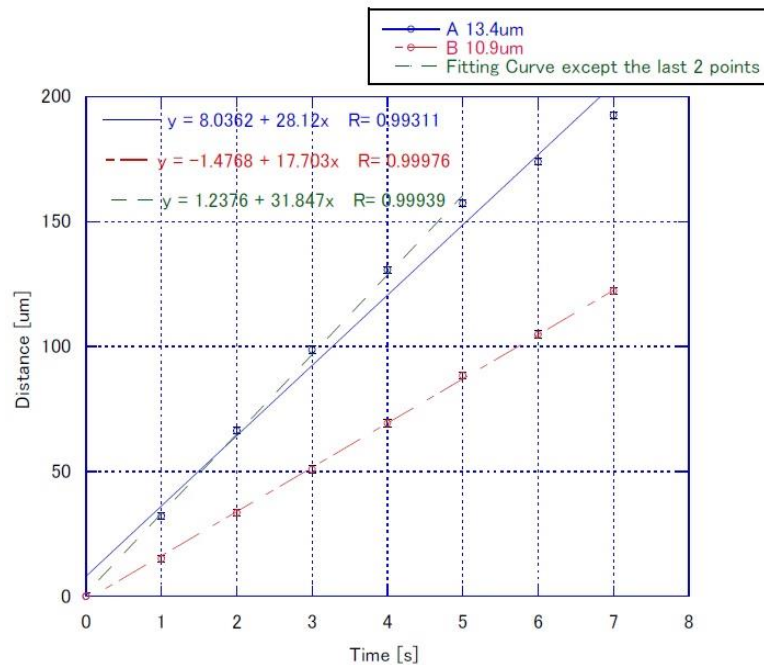


Figure 19: A graph of droplet motions in water as a function of time, $\nabla B = 1.74$ [T/m].

Since it was quite difficult to form the droplets of ferrofluid in water in comparison with glycerine, the data for only two sizes of the droplets was

obtained. According to this graph, the speed of droplet A was reduced from $t = 5$ s. Thus, the value of the speed of droplet A was determined by the fitting curve except for the last two points. The values of the speed, r_{eff} , and r_b can be acquired by using the literature value of the viscosity, $0.890 \text{ mPa}\cdot\text{s}$ (at 25°C) [37][38]. The results are shown in Table 5.

Table 5: The values of Speed, r_{eff} , r_b for each size of the droplets in water.

	A	B
Diameter [μm]	13.4	10.9
Speed [$\mu\text{m} / \text{s}$]	31.8	17.7
r_{eff} [μm]	3.76	2.89
r_b [μm]	2.93	2.56

The values of r_b are $2.93 \mu\text{m}$ and $2.56\mu\text{m}$ for droplet A and droplet B respectively, while the value in glycerine is approximately $1.8 \mu\text{m}$. Table 6 shows the viscosity determined by using $2.7 \mu\text{m}$ as the value of r_b .

Table 6: The values of viscosity for each size of the droplets in water, $r_b = 2.7\mu\text{m}$.

	A	B	Literature Value
Diameter [μm]	13.4	10.9	
Speed [$\mu\text{m} / \text{s}$]	31.8	17.7	
Viscosity [$\mu\text{m} \cdot \text{s}$]	1.06	0.77	0.89

The differences between the literature value and the experimental values are over 10% of the literature value. These errors could be caused by the error of the diameter measurement. According to the theory, the value of viscosity is intensely depending on the diameter size and proportional to the third power of the diameter. The measurement error was $\pm 1.4 \mu\text{m}$, which is over 10 % of the values of the diameter. To take this fact into consideration, there are some possibilities that the differences were caused by such measurement error, and it could be said that the assumption is reasonable.

3-3 Silicone Oil

In this experiment, Magnet B was used and the distance between Magnet B and the centre of the cell was 1.5 cm. It should be noted that water-based ferrofluid was employed in this section. The viscosity of silicone oil employed in this experiment is 50 cSt in CGS system of units, which is 48.6 mPa·s in SI system of units. The motions of the droplets under external magnetic field are shown in Figure 20. The values of the speed, r_{eff} , and r_b were calculated by taking the same steps as the above one, as shown in Table 7.

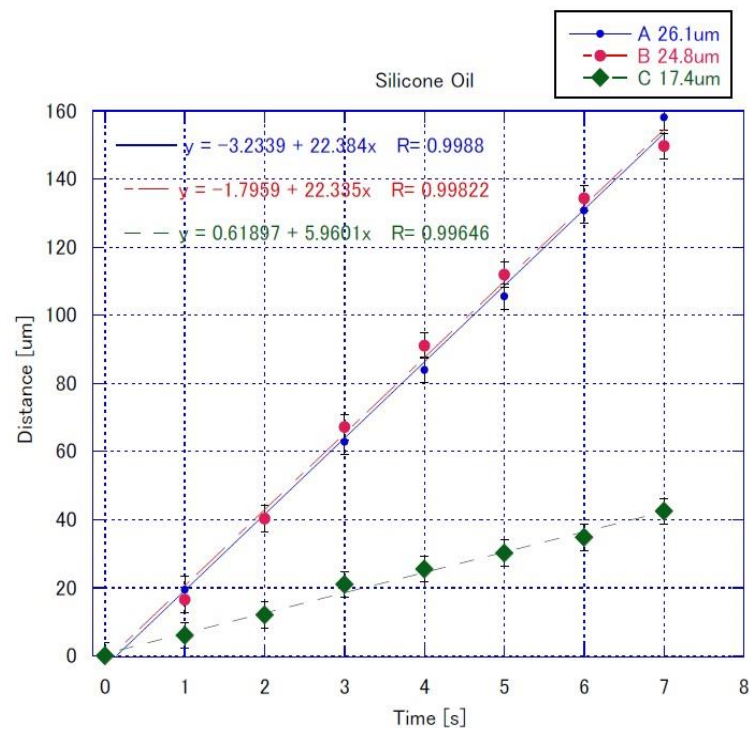


Figure 20: A graph of droplet motions in silicone oil as a function of time, $\nabla B=12.6$ [T/m].

Table 7: The values of Speed, r_{eff} , r_b for each size of the droplets in silicone oil.

	A	B	C
Diameter [μm]	26.1	24.8	17.4
Speed [$\mu\text{m/s}$]	22.4	22.3	5.96
r_{eff} [μm]	8.13	7.98	4.57
r_b [μm]	4.93	4.42	4.13

The values of r_b are quite different from the values for glycerine and water. From this result, r_b could be set as $4.5 \mu\text{m}$. Using this value, the viscosity was determined in the same way, which is shown in Table 8.

Table 8: The values of viscosity for each size of the droplets in silicone oil, $r_b = 4.5 \mu\text{m}$.

	A	B	C	Literature Value
Diameter [μm]	26.1	24.8	17.4	
Speed [$\mu\text{m/s}$]	22.4	22.3	5.96	
Viscosity [mPa·s]	56.6	47.1	37.8	48.6

The differences between the literature value and the experimental values are approximately 20 % of the literature value. In this experiment, the measurement error was $\pm 3.8 \mu\text{m}$, which is much larger than the measurement error in the experiments of water. It could be said that this fact was caused by the measurement errors of the diameter and this experiment requires the accurate measurements.

4 Liquid Crystal Results and Discussion

4-1 Size Dependency

As the first experiment of 5CB-ferrofluid dispersion, the size dependency of the speed of the droplets was researched because the thickness of the boundary layer is required to research the other properties. The steps of this experiment are same as the isotropic experiments, which the motions of three sizes droplets were observed under external magnetic fields and the thickness of the boundary layer was determined by using the equation (12) with literature values of the viscosity and other quantities. In this experiment, Magnet A was used and the distance between Magnet A and the centre of the cell was 2.5 cm. The direction of the applied magnetic field was parallel to the director. The cell gap was at 100 μm and the temperature was 25 °C. The viscosity for parallel direction to the director was named as γ_{\parallel} in this paper, while the viscosity for perpendicular direction to the director was named as γ_{\perp} . The literature value of γ_{\parallel} at 25 °C is approximately 40 mPa·s [14].

The texture of the dispersion is shown in Figure 21. Figure 21 (a) is an entire photo of the dispersion and Figure 21 (b) is an enlarged photo of (a) focusing on one droplet. It can be seen in the photo (b) that the area around the droplets is blurred. This photo shows that the droplet play the role as a defect in the liquid crystal and the director around the droplet cannot be determined. As a result of the experiment, the speed for different sizes of the droplets is shown in Figure 22.

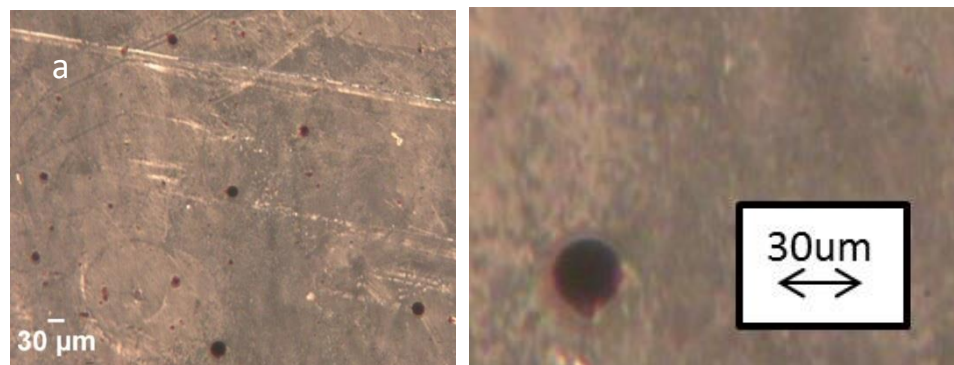


Figure 21: Photos of 5CB-ferrofluid dispersion, (a): an entire phot (b): an enlarged photo

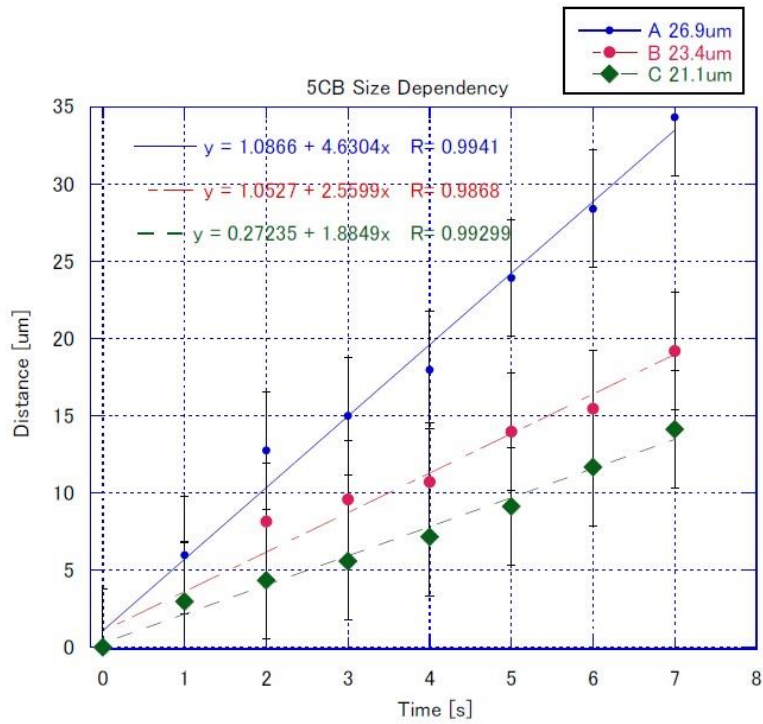


Figure 22: A graph of droplet motions for several sizes in 5CB as a function of time, $\nabla B=1.74[T/m]$.

According to Figure 22, the size dependency which was shown in the section of isotropic liquids can be seen; the larger droplet is moving the faster. The values of the speed, r_{eff} , and r_b were determined by using above mentioned literature values, as shown in Table 9.

Table 9: The values of Speed, r_{eff} , r_b for each size of the droplets in 5CB.

	A	B	C
Diameter [μm]	26.9	23.4	21.1
Speed [$\mu\text{m/s}$]	4.63	2.90	2.24
r_{eff} [μm]	8.79	7.19	6.37
r_b [μm]	4.64	4.50	4.15

According to Table 8, the values of r_b for each size droplet are quite similar to each other. It is reasonable that the thickness of boundary layer is set as $4.5 \mu\text{m}$ since the error for each droplet is $\pm 10 \%$ at most. By using the value, $r_b = 4.5 \mu\text{m}$, the viscosity was determined by the equation (12), which is shown in Table 10.

Table 10: The values of viscosity for each size of the droplets in 5CB, $r_b = 4.5 \mu\text{m}$.

	A	B	C	Literature Value
Diameter [μm]	26.9	23.4	21.1	
Speed [$\mu\text{m/s}$]	4.63	2.90	2.24	
$\gamma_{ }$ [$\text{mPa}\cdot\text{s}$]	41.9	40.0	33.8	40

The values of the viscosity for droplet A, B are quite similar with the literature value, while the difference between the literature value and the value for C is around 20 % of the literature value. There is a high possibility that this error was caused by the measurement error of the diameter. Otherwise, it is a little possible that the droplet C touched to the glass surface and this changed the speed.

In terms of reliability of the value of boundary layer, it was found that the small size droplets did not move under the magnetic fields. Figure 23 shows such behaviour. In Figure 23, the small droplets of size 8 μm did not move while the large droplet of size 26.9 μm moved.

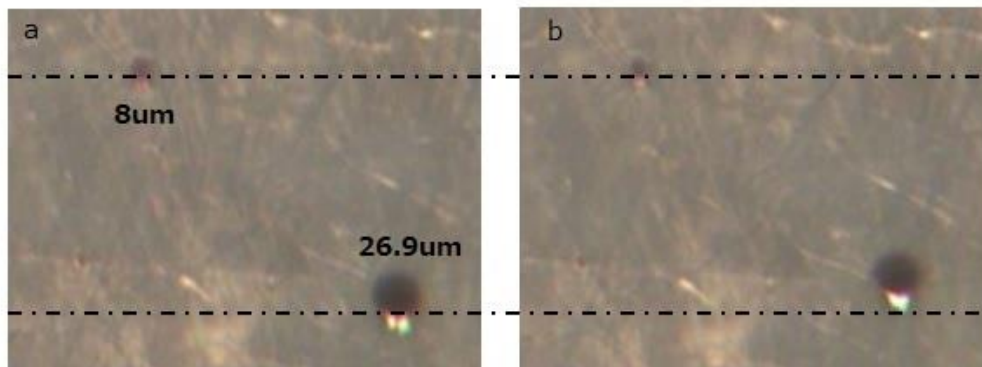


Figure 23: Photos of the motions of the ferrofluid droplets under the magnetic fields, (b) is 5 seconds after the moment of (a).

This fact strongly supports the assumption that there are the boundary layers in the ferrofluid droplets under magnetic fields and its thickness is constant for any size droplets, at 4.5 μm . In the following sections, the value of r_b will be considered as 4.5 μm in order to analyze the several sorts of SCB properties.

4-2 Anisotropy

In this section, the anisotropy of 5CB will be shown by determining γ_{\parallel} and γ_{\perp} with such method. To go into the detail of the experimental steps, the external magnetic field whose direction was parallel to the orientation of the director was applied to the cell, after that, the direction of the magnetic field was changed to be perpendicular to the orientation of the director and repeat the same way. While these steps were taken, the same droplet was focused on and its motion was observed. In this experiment, Magnet A was used and the distance between Magnet A and the centre of the cell was 2.5 cm. The cell gap was at 100 μm and the temperature was 25 $^{\circ}\text{C}$. The motions corresponding to each direction is shown in Figure 24.

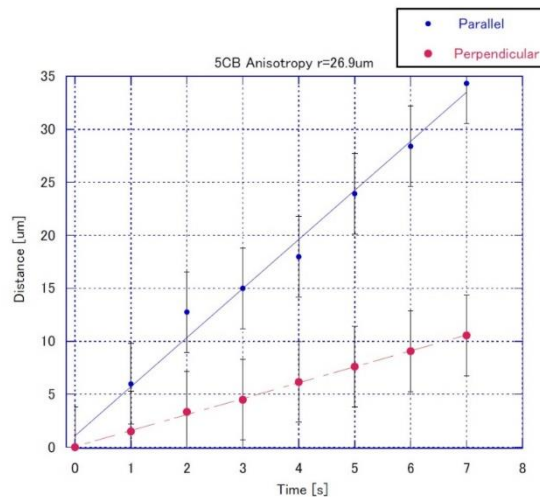


Figure 24: A graph of droplet motions corresponding to each direction of the magnetic field in 5CB as a function of time, $\nabla B=1.74$ [T/m].

It is obvious from Figure 24 that the speed of Parallel is much faster than the speed of Perpendicular, which means γ_{\parallel} is much smaller than γ_{\perp} as the theory. This graph performed the anisotropy of 5CB. The result of the calculation is shown in Table 9.

Table 11: The values of viscosity for each direction, $r_b = 4.5 \mu\text{m}$.

	Parallel	Perpendicular
Diameter [μm]	26.9	26.9
Speed [$\mu\text{m/s}$]	4.63	1.50
γ [$\text{mPa}\cdot\text{s}$]	41.8	129

The literature values of γ_{\parallel} and γ_{\perp} at 25 °C are 40 mPa·s and 120 mPa·s [14], shown in Figure 25. In Figure 25, the viscosity data was collected with the viscometer by Chmielewski. Three factors, η_1 , η_2 , and η_3 , were based on Miesowicz's work, which they could be independently measured experimentally by considering the orientation of the director in relation to the flow velocity [12]. If the viscometer is used, where LCs are covered by two surface and applied with distortion on the one surface while the other one is fixed, the flow is occurred in LCs and its velocity direction should be parallel to the distortion direction and its

acceleration should be perpendicular to the two surface. η_1 means the viscosity when the director is parallel to the direction of the flow velocity, while η_2 is the viscosity when the director is parallel to the direction of the gradient of the flow velocity, and η_3 is the viscosity when the director is perpendicular to both of them[35]. In this experiment, η_1 and η_3 are corresponding to γ_{\parallel} and γ_{\perp} respectively if it is assumed that the flow direction is same as the droplet motion direction . In comparison with the literature values, it could be said that the experimental values are reasonable. This result also supports the reliability of this method and the equation (12).

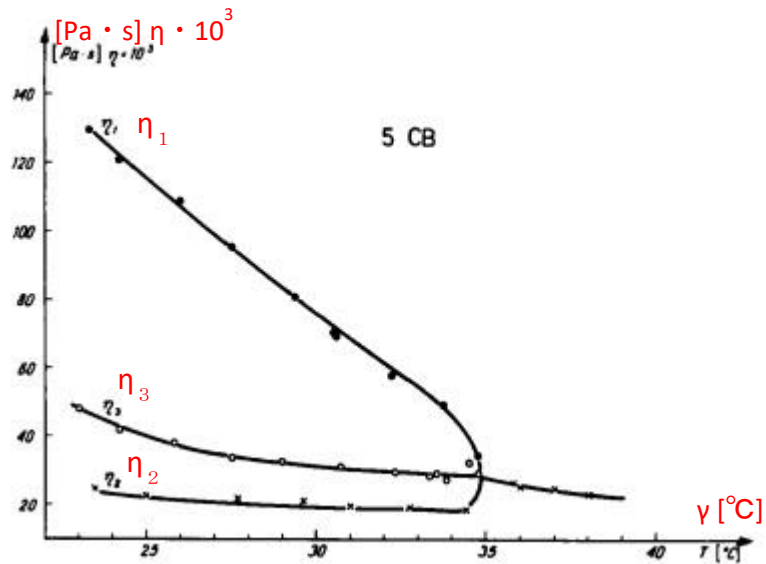


Figure 25: A graph of temperature dependence of the viscosity coefficients for 5CB [14] (adding red coloured letters for visibility).

4-3 Different Strength of Magnetic Field

This experiment was aimed to observe the behaviour of the droplets for the different strength of magnetic fields. In this experiment, Magnet A was used and the distance between Magnet A and the centre of the cell was changed from 3.0 cm to 1.5 cm by intervals of 0.5 cm. These several strengths of the magnetic fields were applied to one droplet and its motion was observed. The direction of the applied magnetic field was parallel to the director. The cell gap was at 100 μm and the temperature was 25 $^{\circ}\text{C}$. Figure 26 shows the speed of the droplets versus the strength of the magnetic field.

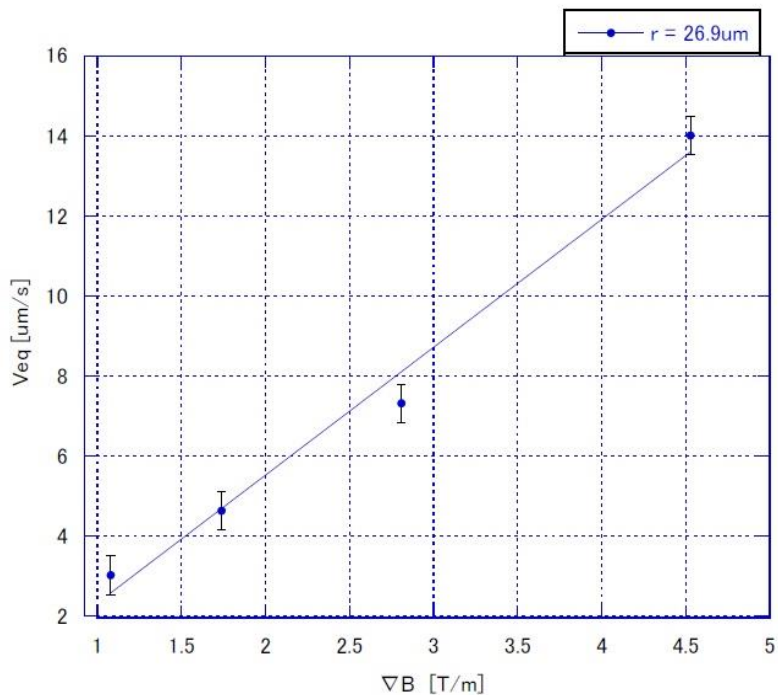


Figure 26: A graph of speed of the droplet in 5CB as a function of ∇B .

It can be observed from Figure 26 that the shape of this graph is quite similar to the linear shape, which means that the results are following the relationship between v_{eq} and ∇B in the equation (12) as expected. At the same time, this result provides the fact that the droplet motions in 5CB are not depending on the strength of the magnetic fields. The viscosity determined with this data is shown in Table 12.

Table 12: The values of viscosity for each strength of magnetic field, $r_b = 4.5 \mu\text{m}$.

	A	B	C	D
Diameter [μm]	26.9	26.9	26.9	26.9
∇B [T]	1.08	1.74	2.81	4.53
Speed [$\mu\text{m} / \text{s}$]	3.85	4.63	7.32	16.9
$\gamma_{ }$ [mPa·s]	39.8	41.9	42.8	36.0

We obtained the results which are similar to the literature value, $\gamma_{||} = 40 \text{ mPa} \cdot \text{s}$. From this result, it can be said that the thickness of the boundary layer is independent of the strength of the magnetic field.

4-4 Gap Dependency

This experiment was aimed to observe the behaviour of the droplets for different sizes of the cell gap. In this experiment, three sizes of the cell gap were prepared: 55 μm , 100 μm , 220 μm . In terms of the diameter, since three types of cells were prepared, the different droplets which have similar values of the diameter with each other were focused on. Magnet A was used and the distance between Magnet A and the centre of the cell was 2.5 cm. The direction of the applied magnetic field was parallel to the director. The temperature was 25 $^{\circ}\text{C}$. Table 13 shows the values of all kinds of notable quantities and the viscosity.

Table 13: The values of viscosity for each cell gap, $r_b = 4.5 \mu\text{m}$.

	A	B	C
Gap [μm]	55	100	220
Diameter [μm]	26.9	26.9	26.6
Speed [$\mu\text{m} / \text{s}$]	5.18	4.63	4.13
γ_{\parallel} [mPa·s]	37.7	41.8	45.1

There are relatively small differences between the values. The trends which the larger cell gap shows the higher viscosity can be found. It can be assumed that this trend is caused by the relationship between the cell gap and anisotropy of the sample. In the case of preparing the cell which has the larger cell gap, it is more difficult to obtain the perfect alignment of molecules in liquid crystal between two glass plates than in the case of the smaller gap. Because of this, in the less ordered cell, there are larger components in γ_{\perp} than in the well-ordered cell. Hence, the larger cell gap shows the higher viscosity. This result describes obviously that liquid crystals become less ordered as the cell gap is increased.

4-5 Temperature Dependency

In this section, it was aimed to observe the thermotropic behaviour of 5CB concerning anisotropy and determine the values of γ_{\parallel} and γ_{\perp} at several temperatures in a certain range. As an additional equipment, the hot stage (FP90, Mettler Toledo, UK) was used to heat or cool the cell. After the cell temperature reached to the certain value, the magnetic field was attached to the iron exterior wall of the hot stage and applied to the cell. In terms of the magnet, Magnet B was used and the distance between Magnet B and the centre of the cell was 3.0 cm. Five different values of temperature were used in this experiment, such as 26, 29, 32, 34, 36 °C. The same droplet had been employed for each temperature and the cell gap was 100 μm .

Figure 27 shows the texture of the dispersion at several values of temperature. These photos were taken under cross polarized light. It is clear that 5CB showed the nematic phase until 34 °C in Figure 27 (a-d). At 36 °C, 5CB changed to isotropic liquid and its texture was changed into the dark under the cross-polarized light as shown in Figure 27 (e).

Figure 28 shows the motions of the droplet as a function of time at several temperatures. As the temperature is increasing, the slope of the linear fitting for

the perpendicular direction is approaching to the slop for the parallel direction.

This behaviour indicates that the molecules in 5CB were losing their order as the temperature was increasing. This fact corresponds with the previous studies [14].

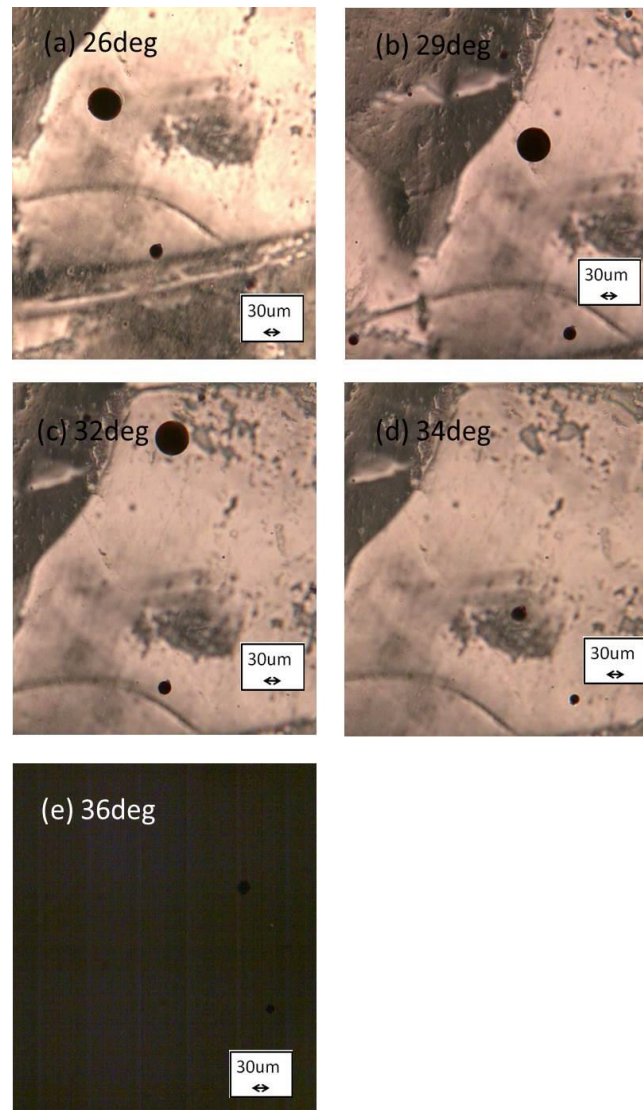


Figure 27: Photos of 5CB-ferrofluid dispersion under cross polarized light at several temperatures.

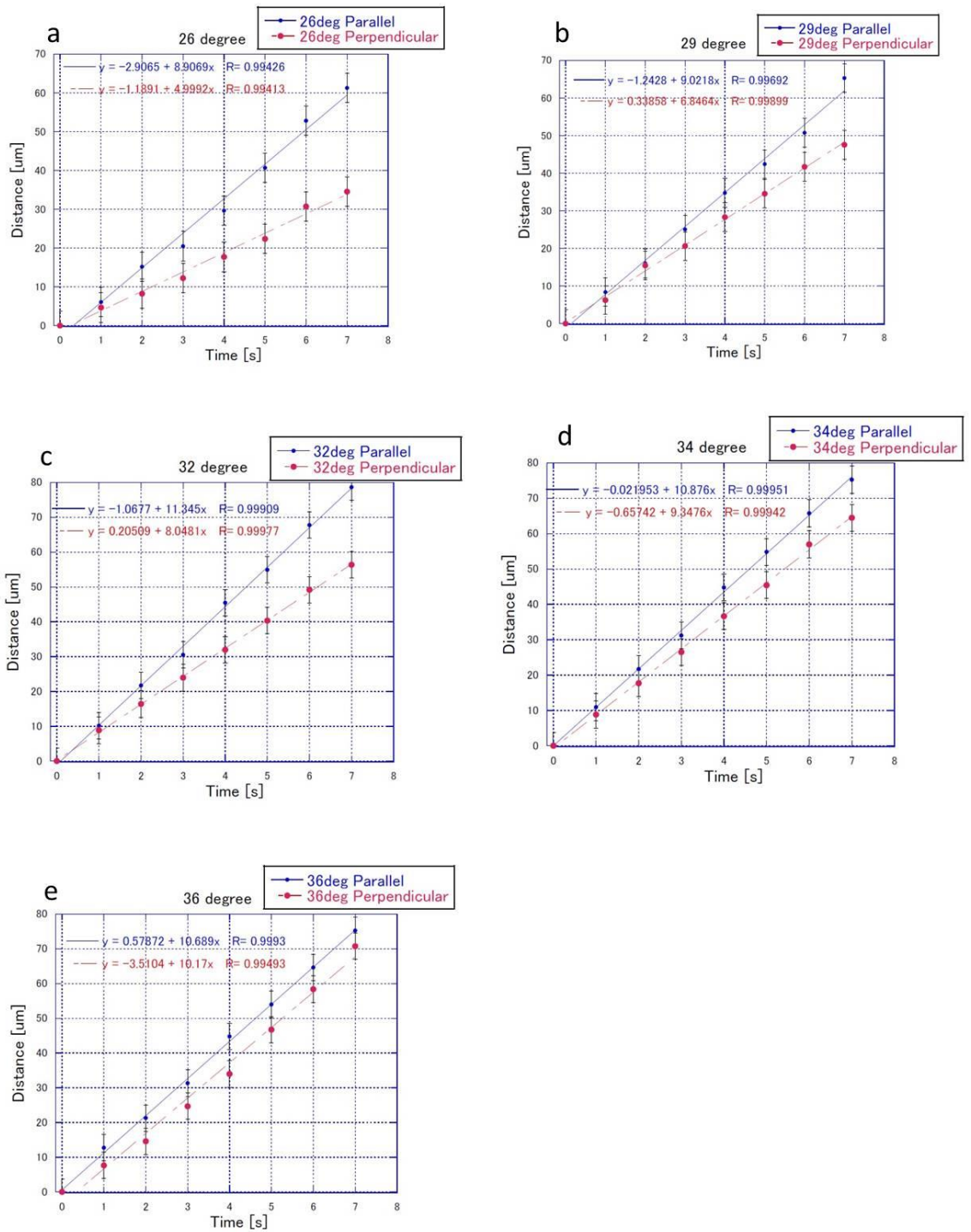


Figure 28: Graphs of droplet motions at several temperatures in 5CB as a function of time, $\nabla B = 2.92$ [T/m].

As a result, the data is shown in Table 14. And Figure 29 shows the viscosity versus temperature based on the data of Table 14.

Table 14: The values of viscosity for each temperature, $r_b = 4.5 \mu\text{m}$.

Temp [°C]	26	29	32	34	36
Diameter [μm]	26.9	26.9	26.9	26.9	26.9
Parallel Speed [$\mu\text{m} / \text{s}$]	8.91	9.02	11.3	10.9	10.7
γ_{\parallel} [mPa·s]	36.3	36.1	28.7	29.9	30.5
Perpendicular Speed [$\mu\text{m} / \text{s}$]	4.99	6.85	8.05	9.37	10.2
γ_{\perp} [mPa·s]	64.7	47.5	40.4	34.7	32.0

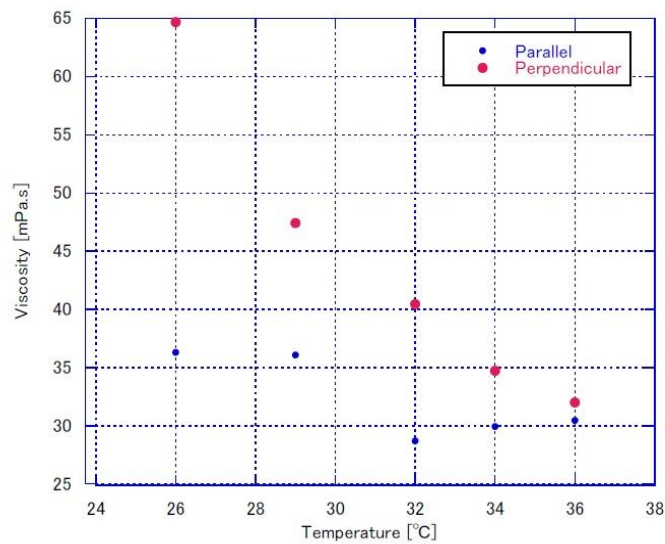


Figure 29: A graph of the viscosity of 5CB as a function of temperature

This graph shows the thermotropic behaviour of the viscosity well, and we can see that the anisotropy was decreasing as the temperature was increased. At 36 °C, the value of γ_{\perp} became to be quite similar with the value of γ_{\parallel} , which means 5CB became the isotropic liquid as the previous study showed [14]. In comparison with the literature values which are shown in Figure 25, the experimental values of γ_{\perp} are lower than the literature values at 26-34 °C, while the experimental values of γ_{\parallel} are similar with the literature values. There is a high possibility that the way to apply the magnetic fields causes such error. The magnetic field was applied to the cell in the situation that the magnet was attached to the iron exterior wall of the hot stage. This step made the exterior wall magnetized and changed the direction of the magnetic field since the hot stage was surrounded by the four side exterior wall. It means that some of the parallel components of the magnetic field to the director of 5CB were applied to the cell when the perpendicular direction was measured. This parallel component possibly had influences on γ_{\perp} , while the perpendicular component had less influence on γ_{\parallel} since $\gamma_{\parallel} < \gamma_{\perp}$. It is quite difficult to relate it to the temperature effect on the ferrofluids because Section 4.2 showed the experimental values which is quite similar with the literature value at 25 °C.

5 Conclusion and Outlook

To conclude the isotropic liquids – ferrofluids dispersion, the method to determine the viscosity of liquids by observing the motions of the droplets under the magnetic fields was established with the assumption that the droplets involve the boundary layers. It could be said from the results that the assumption is reasonable. The values of the viscosity are intensely depending on the diameter of the droplets, thus, the accurate measurement is required.

Through the experiment of 5CB – ferrofluids dispersion, it was found that the method used for the isotropic is useful for 5CB as well and leads us to obtain the anisotropy behaviour of the viscosity of 5CB. The values of the anisotropy experiments are quite similar with the values of the previous study which was measured by the viscometer, and the method is possible to be reliable. The behaviour of the ferrofluids forming the boundary layers was observed by the picture, the droplet which had a smaller diameter than the thickness of the boundary layers did not move under the magnetic field while the larger droplet moved. This result is the evidence for the assumption. The fact that boundary layer is independent of the strength of the magnetic fields was discovered by observing the droplet motions under different strengths of the magnetic fields.

Regarding to the cell gap dependency, the behaviour that 5CB is losing its anisotropy as the cell gap is increased was observed with quantitate data.

Although the results of temperature dependency included the error which is expected to be caused by the measurement step, the behaviour that 5CB is losing its anisotropy as the temperature is increased was observed.

In summary, this new method to determine the viscosity was established and works well for 5CB. This methods will leads us to observe the various kinds of anisotropy properties of the nematic liquid crystals with the quantitate aspects.

For further studies, the accuracy of the measurement will be required to be increased. In this method, there is a high possibility to cause the error because measuring the motions of the droplets is conducted by a hand with the imaging software although the scale is micro-sized. Then, this method is expected to be applied to the other liquid crystal system and to be a new method to determine the liquid crystal phase and properties with the quantitate aspects eventually. In particular, some of the liquid crystal phases are quite hard to be distinguished from the others with observing the microscope texture and this method is possible to be a new way to distinguish it.

Acknowledgements

I would like to thank Dr. Ingo Dierking for his great support throughout my project. I also would like to thank Prof. Anne Juel for her support as my cosupervisor and Shakhawan Al-Zangana for his demonstrations and help in the beginning of this project.

Reference

- [1] I. C. Khoo, (2007), *Liquid Crystals*, John Wiley & Sons, Inc..
- [2] T. J. Sluckin, D. A. Dunmur, H. Stegemeyer, (2004), *Crystals That Flow: Classic Papers from the History of Liquid Crystals (Liquid Crystals Book Series)*, CRC Press.
- [3] J. A. Castellano, (2005), *Liquid Gold: The Story of Liquid Crystal Displays and the Creation of an Industry*, World Scientific Publishing Co. Pte. Ltd.
- [4] J. Beeckman, K. Neyts, P. J. M. Vanbrabant, (2011), *Liquid-crystal photonic applications*, *Optical Engineering*, **50**, 081202.
- [5] M. Mitov , N. Dessaud, (2006), *Going beyond the reflectance limit of cholesteric liquid crystals*, *Nature*, **5**, 361.
- [6] P. J. Collings, M. Hird, (1997), *Introduction to Liquid Crystals: Chemistry and Physics*, CRC Press.
- [7] D. C. Zografopoulos, R. Asquini, E. E. Kriezis, A. d'Alessandro, R. Beccherelli,(2012), *Guided-wave liquid-crystal photonics, Lab on a chip*,**12**, 3598.

- [8] S. S. Papell, (1965), *Low viscosity magnetic uid obtained by the colloidal suspension of magnetic particles*, US Patent: US3215572 A.
- [9] S. Odenback, (2009), *Colloidal Magnetic Fluids*, Springer eBooks.
- [10] P. Poulin, H. Stack, T. C. Lubensky, D. A. Weitz, (1997), *Novel colloidal interactions in anisotropic fluids*, *Science*, **275**, 5307, 1770.
- [11] P. Poulin, V. Cabuil, D. A. Weitz, (1997), *Direct Measurement of Colloidal Forces in an Anisotropic Solvent*, *Phys. Rev. Lett.*, **79**, 24, 4862.
- [12] M. Miesowicz, (1936), *Der Einflub des magnetischen Feldes auf die Viskositat der flussigkeiten in der nematischen Phase*, *Bul. Acad. Pol. A*, 228
- [13] M. Miesowicz, (1946), *The Three Coefficients of Viscosity of Anisotropic Liquids*, *Nature*, **158**, 27
- [14] A. G. Chimielewski,(1986), *Viscosity Coefficients of Some Nematic Liquid Crystals*, *Mol. Cryst. Liq. Cryst.*, **132**, 339.
- [15] F. Schneider, H. Knepe, N. K. Sharma, (1981), *A Comparative Study of the Viscosity Coefficients of Some Nematic Liquid Crystals*, *Bet. Bunsenges. phys. Chem.*, **85**, 784.
- [16] S. Chandrasekhar, (1977), *Liquid crystals*, Cambridge University Press.
- [17] I. Khoo, S. Wu, (1993), *Optics and nonlinear optics of liquid crystals*. World Scientific.

- [18] D. A. Dunmur, A. Fukuda, G. R. Luckhurst, (2001), *Physical properties of liquid-crystals: nematics*, An INSPEC Publication.
- [19] R. A. L. Jones, (2002), *Soft Condensed Matter*, Oxford University Press.
- [20] S. M. Shamid, S. Dhakal, J. V. Selinger, (2013), *Statistical mechanics of bend flexoelectricity and the twist-bend phase in bent-core liquid crystals*, *Physical Review E*, **87**, 5, 052503.
- [21] G. Andrej, S. Kralj, (2009), *Topological Defects in Liquid Crystals*, Society for Experimental Mechanics Inc.
- [22] I. Muševič, M. Škarabot, U. Tkalec, M. Ravnik, S. Žumer, (2006), *Two-dimensional nematic colloidal crystals self-assembled by topological defects*, *Science*, **313**, 5789, 954.
- [23] W. Brinkman, P. Cladis, (1982), *Defect in Liquid Crystals*, *Physics Today*, **35**, 48.
- [24] T. Kelly, (2015), *MPhys Project: Colloidal Interactions of Ferrofluid Droplets in a Nematic Liquid Crystal*, University of Manchester.
- [25] P. Poulin, D. A. Weitz, (1998), *Inverted and multiple nematic emulsion*, *Phys. Rev. E*, **57**, 626.

- [26] O. Mondain-Monval, J. C. Dedieu, T. Gulik-Krzywicki and P. Poulin, (1999), *Suspension of spherical particles in nematic solutions of disks and rods*, Eur. Phys. J. B, **12**, 167.
- [27] I. Musevic, (2013), *Nematic colloids, topology and photonics*, Phil Trans R Soc A, **371**, 20120266.
- [28] E. M. Terentjev, (1995), *Disclination loops, standing alone and around solid particles, in nematic liquid crystals*, Phys. Rev. E, **51**, 1330.
- [29] S. Odenbach, (2002), *Ferrofluids*, Springer.
- [30] S. Odenbach, (2002), *Magnetoviscous Effects in Ferrofluids*, Springer.
- [31] Tesla Downunder, <http://tesladownder.com>, (24th, Sep, 2017).
- [32] H. Li, Y. Wu, X. Wang, C. Zhu, T. Fu, Y. Ma, (2016), *Magnetofluidic control of the breakup of ferrofluid droplets in amicrofluidic Y-Junction*, RSC Adv., **6**, 778.
- [33]W. S. Rasband, ImageJ, U. S. National Institutes of Health, Bethesda, Maryland, USA, <http://imagej.nih.gov/ij/>, (24th, Sep, 2017).
- [34]C. A. Schneider, W. S. Rasband, K. W. Eliceiri,(2012), *NIH Image to ImageJ: 25 years of image analysis*, Nature Methods, **9**, 671.

- [35] I. W. Stewart, (2004), *The Static and Dynamic Continuum Theory of Liquid Crystals*, Taylor & Francis.
- [36] S. Adio, M. Sharifpur, J. Meyer, (2013), *Investigation into Effective Viscosity and Electrical Conductivity of γ -Al₂O₃-Glycerol Nanofluids in Einstein Concentration Regime*, UKHTC2013, 92, 1.
- [37] J. B. Segur, H. E. Oberstar, (1951), *Viscosity of Glycerol and Its Aqueous Solutions*, Industrial and Engineering Chemistry, 49, 2117.
- [38] National Astronomical Observation of Japan, (2016), *Chronological Scientific Tables*, MARUZEN-YUSHODO Co., Ltd.